Science of Sintering, **38** (2006)117-123

DOI: **10.2298/SOS0602117J**

UDK 537.533.35:77.026.34

Subwavelength Hole Arrays with Nanoapertures Fabricated by Scanning Probe Nanolithography

Z. Jakšić[*)], **M. Maksimović, D. Vasiljević-Radović, M. Sarajlić**
IHTM – Centre of Microelectronic Technologies and Single Crystals, Belgrade, Serbia

Abstract:

Owing to their surface plasmon-based operation, arrays of subwavelength holes show extraordinary electromagnetic transmission and intense field localizations of several orders of magnitude. Thus they were proposed as the basic building blocks for a number of applications utilizing the enhancement of nonlinear optical effects. We designed and simulated nanometer-sized subwavelength holes using an analytical approach. In our experiments we used the scanning probe method for nanolithographic fabrication of subwavelength hole arrays in silver layers sputtered on a positive photoresist substrate. We fabricated ordered nanohole patterns with different shapes, dispositions and proportions. The smallest width was about 60 nm. We characterized the fabricated samples by atomic force microscopy.

Keywords*: Nanooptics, Surface plasmons, Subwavelength hole arrays, Nanofabrication, Nanolithography, Atomic force microscopy.*

1. Introduction

Extraordinary optical transmittance through subwavelength hole arrays was described in the seminal paper by Ebbesen et al [1] and subsequently analyzed in many papers [2-6]. If an optically thick (opaque) metallic perforated film with an ordered or disordered array of holes is illuminated by optical radiation with a wavelength much larger than the holes, it transmits an extraordinarily large portion of the incident radiation, although according to the conventional Bethe-Bowcamp theory [7-8] no radiation should be transmitted at all. This phenomenon comes from surface plasmon polaritons (SPP) appearing on the surface of the metallic film as a result of the incident electromagnetic field exciting surface electrons and coupling with them. The SPP may be either localized or propagating and are excited by a incident electromagnetic wave if their wavelengths coincide. Along the z-axis the SPP are evanescent, i.e. decay exponentially in both directions. Subwavelength hole arrays are similar in their function to the frequency selective surfaces, FSS [9]

Fig. 1 shows the metal film with an array of holes, which may be of an arbitrary shape and layout, illuminated by a normally incident plane electromagnetic wave. The metal film is thick enough to serve as an opaque screen that does not transmit light, and the holes are much smaller than the operating wavelength. Additionally, an array of grooves or

[*)] Corresponding author: jaksa@nanosys.ihtm.bg.ac.yu

corrugations may exist on the surface. Both holes and corrugations serve as a modulation to the metallic film surface, since an electromagnetic wave cannot excite SPP on a perfectly smooth and flat surface. When the electromagnetic wave arrives, it is combined with charge carriers into a SPP on the surface; the SPP are transmitted through the holes. During transmission, their complete energy is localized to the subwavelength apertures and thus intensified several orders of magnitude. At the other side of the sample, the SPP break apart again into electron states and a propagating electromagnetic wave. As a result sharp resonance peaks in transmission appear at wavelengths exceeding by far the spatial dimensions of the holes.

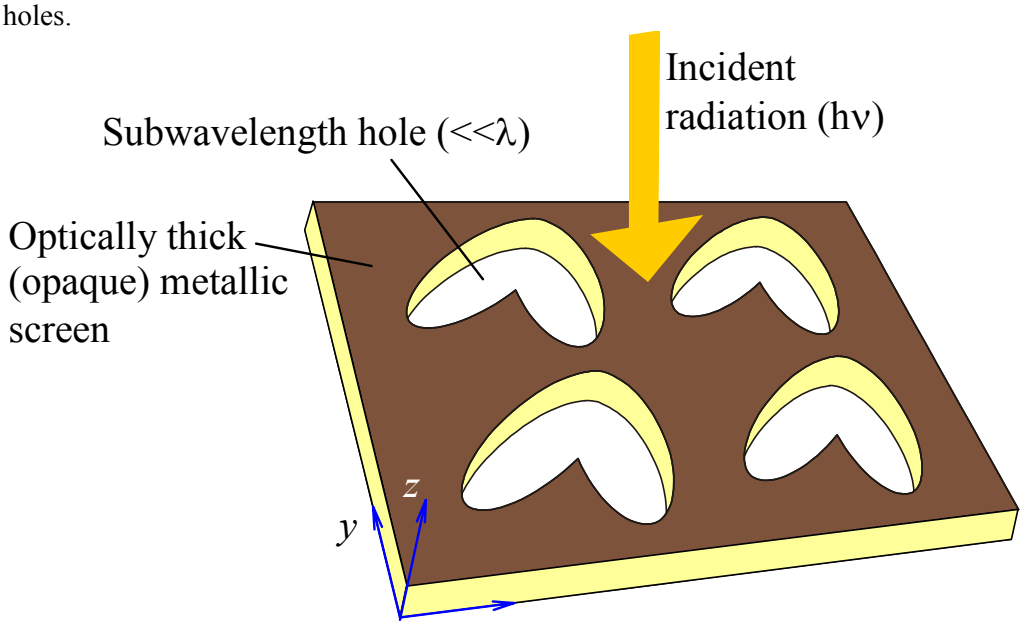

Fig. 1. Ordered subwavelength hole array with an arbitrary shape of holes.

Extraordinary optical transmittance through subwavelength holes is of large practical importance for different nanophotonic applications. Strong localization of the fields within the holes, which may exceed several orders of magnitude, appears especially important, since it could be used for practical implementation of nonlinear optical effects requiring exceedingly strong fields, and ultimately for the fabrication of all-optical active devices [10-11].

In this paper we experimentally consider the use of scanning-probe based nanolithography as a method of fabrication of subwavelength hole arrays. This simplifies procedures for array prototyping and drastically reduces both the cost and the time needed to fabricate experimental structures.

2. Calculation of transmittance of nanoholes

Most papers on nanohole transmission are either dedicated to a purely experimental investigation of the phenomenon or to calculation of extraordinary transmission using numerical simulation, typically either by a finite difference time domain or finite element analysis [12-13]. In this paper we utilize an analytical model based on the generalized Ohm law approximation or GOL [1] and apply it to the case of a metal film with nanoholes in a manner similar to that in [15]. The electric field in a nanohole is calculated exploiting the percolation theory and Maxwell-Garnett approximation [16] and enables a qualitative assessment of fields in the nanohole array and its spectral transmission.

The geometry of the structure is shown in Fig. 2. A monochromatic plane electromagnetic wave at a wavelength λ, is incident normally to the metal surface. Its electric

and magnetic field components depend only on x and y coordinates. The metal film thickness is *d*, whereas the characteristic spatial scale of nanoholes is *a*, where $a<<\lambda$. The number of the holes is relatively small, i.e. their area is much smaller than the total area of the metal film.

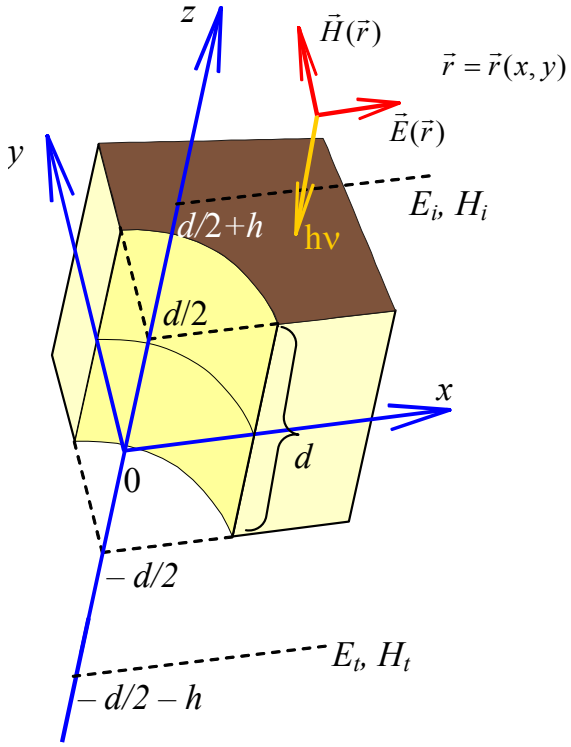

Fig. 2. Problem geometry.

Let us denote by E_i and H_i the electric and magnetic fields at a height *h,* above the upper surface (*i* means 'incident') and by E_t, H_t the transmitted fields at a distance *h,* below the bottom surface. The fields are only dependent on *x* and *y* coordinates, but not on *z* and are monochromatic plane waves, $\exp[i(kx-\omega t)]$. We assume that ε and μ (permittivity and permeability) are scalar variables. The Faraday and Ampere law can then be approximated as

$$\left[\vec{n}_z\times\left(\vec{E}_t(\vec{r})-\vec{E}_i(\vec{r})\right)\right]=i\vec{k}\vec{B}(\vec{r}),\quad \left[\vec{n}_z\times\left(\vec{H}_t(\vec{r})-\vec{H}_i(\vec{r})\right)\right]=i\vec{k}\vec{D}(\vec{r}) \tag{1}$$

where n_z={0,0,1}is an unit vector normal to the plane of the film and *k* is the wave vector. If we introduce $\vec{E}=\vec{E}_i+\vec{E}_t$ (and the same for $\vec{B},\vec{D},\vec{H}$) the generalized Ohm law is

$$\vec{D}(\vec{r})=u(\vec{r})\vec{E}(\vec{r})/k,\quad \vec{B}(\vec{r})=v(\vec{r})\vec{H}(\vec{r})/k \tag{2}$$

where *u* and *v* are Ohmic parameters dependant on the metal film geometry.

Upon averaging (eq. 1) over the whole metal film plane, introducing the effective (averaged) Ohmic parameters as $u_{eff}<\vec{E}>=<u\vec{E}>$, $v_{eff}<\vec{H}>=<v_e\vec{H}>$ and utilizing the connection between the incident and the transmitted fields via the complex transmittance *t* we obtain that the transmission through the film is [15]:

$$T=|t|^2=\left|\frac{1+u_{eff}v_{eff}}{(i+u_{eff})(i+v_{eff})}\right|^2 \tag{3}$$

Next we need to know the effective values of generalized Ohmic parameters in the metal (let us denote it by a subscript *m*) and in holes (subscript *h*). According to the Maxwell-Garnett approach

$$E_h = \frac{2E_m u_m}{u_m + u_h},\ E_m = (E_i + E_t)_m \tag{4}$$

$$u_{eff} = \frac{(1-p)u_m E_m + pu_h E_h}{(1-p)E_m + pE_h},\quad v_{eff} = \frac{(1-p)v_m E_m + pv_h E_h}{(1-p)E_m + pE_h} \tag{5}$$

where p is the concentration of holes on the surface – "fill factor" (here p<<1).

The generalized Ohmic parameters are calculated as

$$u_h = \frac{k\tan(2hk) - \sqrt{\kappa^2 - k^2}\ \tanh[b\sqrt{\kappa^2 - k^2}]}{k + \tan(2hk)\sqrt{\kappa^2 - k^2}\ \tanh[b\sqrt{\kappa^2 - k^2}]}$$

$$u_h = \frac{\tan(2hk)\sqrt{\kappa^2 - k^2} + \tanh[b\sqrt{\kappa^2 - k^2}]}{\sqrt{\kappa^2 - k^2} - k\tan(2hk)\ \tanh[b\sqrt{\kappa^2 - k^2}]} \tag{6}$$

$$u_m = -\cot(hk)\ ,\qquad v_m = -\tan(hk),\qquad b = d/2 - h \tag{7}$$

where n is the complex refractive index of metal and κ is the eigenvalue of the basic mode in a waveguide whose cross-section is identical to the nanohole shape; for instance, κ=3.68/a for a cylindrical hole where a is the hole diameter. If holes are "thin" enough (as in our case) so that d<2h, we can obtain a simplified expression for spectral transmission as

$$T = \sum_j \frac{4p^2 \sin^4\left(\frac{2h\pi}{4h+d} j\right)}{4p^2 \sin^4\left(\frac{2h\pi}{4h+d} j\right) + (4h+d)^2\left(k - \frac{\pi}{4h+d} j + \frac{p}{4h+d}\sin\left(\frac{4h\pi}{4h+d} j\right)\right)^2} \tag{8}$$

where k is the wave vector and j=1,2,3….. are integer values.

Fig. 3 shows qualitative prediction of transmission calculated according to eqs. 2-8.

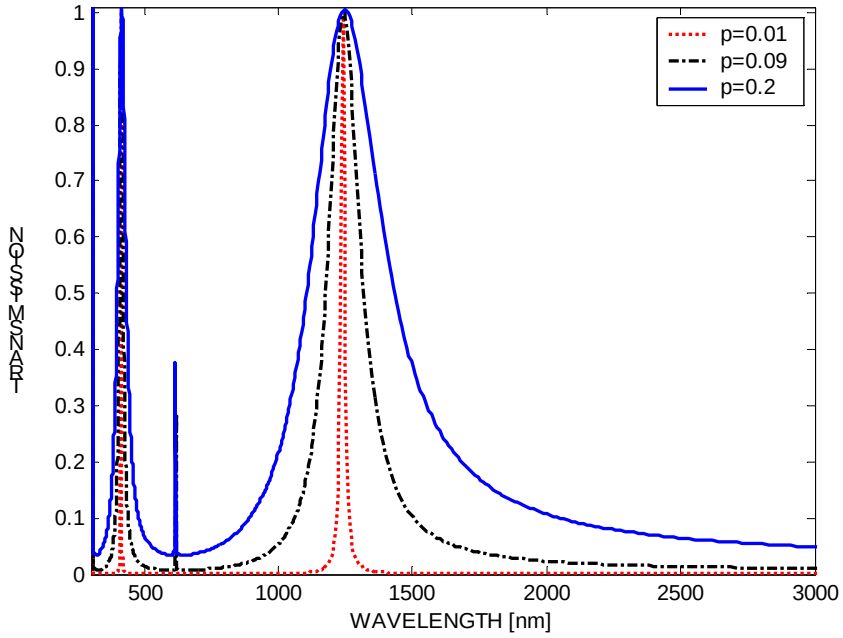

Fig. 3. Spectral transmission of a nanohole array with a square matrix layout of circular holes, d/a=0.08, h/a=0.6

3. Experimental

The substrate for our samples was a double polished single crystalline silicon wafer. The first technological step was to rinse the wafer and to spin-coat it by a positive photoresist 400 nm thick. The resist layer was dried without baking, to avoid unnecessary hardness. The samples were entered into the sputtering chamber and RF sputtered until a 20 nm thick silver layer was deposited over the photoresist.

Prior to our fabrication experiments, we characterized the surface morphology of the samples with the help of atomic force microscopy. It was found that the flatness of the silver surface was better than 2 nm.

The nanolithography experiments were carried out under normal atmospheric pressure and at room temperature. No humidity control was done. Vibration- and shock-free conditions were ensured by an anti-vibration table unit with active oscillation dumping.

To fabricate nanohole arrays we used scanning probe nanolithography on a Veeco Autoprobe CP-Research atomic force microscope (AFM). We used z-scanner movement ('scratching' mode). A silicon nitride microcantilever was used for the operation. The scanner base position was adjusted to 0.9 μm below the zero position, i.e. the scanning probe tip was pressed against the sample surface with a force of several nN. This force was sufficient to 'dig' a groove in the silver layer, while the resist sublayer served as an elastic limiter to the probe tip.

We performed a number of experiments to test the dependence of the depth and width of the obtained nanolithographic lines on the force of the z-scanner movement, but also on the needle tip shape, sample surface material and the needle tip speed.

4. Results and discussion

The z-scanner movement nanolithography makes a 'scratch' in the sample surface, leaving 'upturned' material on its edges. Depending on the scratch depth, this either makes a modulation of the surface or completely breaks it, leaving a hole. As mentioned in section 1, both of these are convenient for making surface plasmon enhanced transmission.

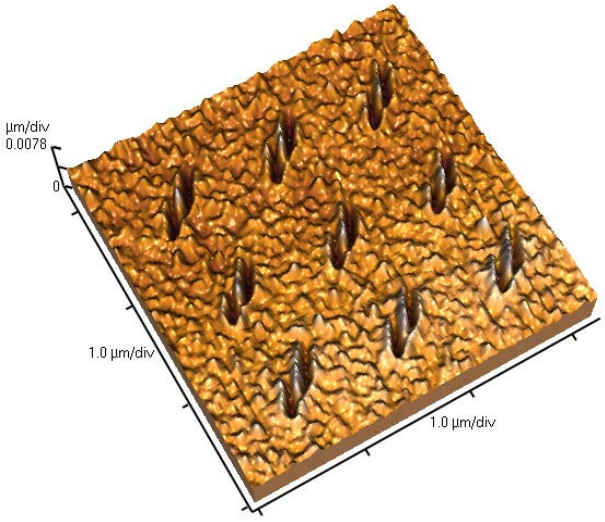

Fig. 4. AFM profile of a nanohole array in a silver film fabricated by z-scanner movement nanolithography.

The z-scanner displacement in our experiments was –0.7 μm, resulting in a nanolithographic line width of about 60 nm. A silver layer on the positive photoresist

substrate was readily formed by the silicon nitride needle tip. Fig. 4 shows a profile of a square matrix of subwavelength holes we formed by z-scanner nanolithography. Each hole is asymmetric, V-shaped, with 150-300 nm width and about 500 nm length.

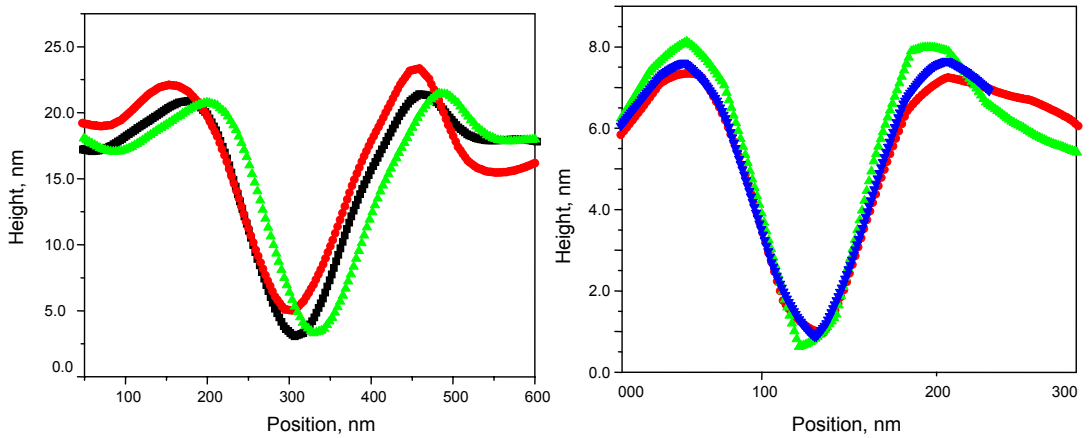

Fig. 5. Profiles of scanning probe-fabricated nanolithographic lines. Different colors denote depth profiles at different positions along a single subwavelength structure

Fig. 5 shows the profiles of nanolithographic lines in different experiments. The depth of the fabricated holes ranged from 6 to 25 nm. We also worked with polycarbonate substrates, where the achieved depth was up to 80 nm.

During our work with nanohole array fabrication we noted gradual 'shifting' of the fabricated patterns during the process in comparison to the designed dimensions. In some samples whole rows of holes were displaced for 60-150 nm. Repeatability was tested by nanofabricating several identical structures and it also ranged between 60 and 150 nm. Also, in some cases besides the designed pattern an additional line up to 200 nm appeared at the beginning, probably as a result of the operation of the piezo-actuated micropositioner. However, according to the analytical model in Section 2, these deviations insignificantly influence the overall performance of the subwavelength hole array, while the most important factor is the shape of the nanoholes. This conclusion is in agreement with literature [4]

5. Conclusion

In our experiments we used scanning-probe based nanolithography to produce subwavelength hole arrays. This simplifies procedures for array fabrication when producing single and unique experimental structures and drastically reduces both their cost and the necessary periods of time in comparison to conventional lithographic and dry etching methods for batch production. Thus we propose its use as a fast prototyping tool for different arrays and shapes of nanoholes for extraordinary optical transmittance. Our next efforts will be dedicated to electromagnetic characterization of samples with subwavelength holes.

References

1. T. W. Ebbesen, H. J. Lezec, H. F. Ghaemi, T. Thio, P. A. Wolff, Nature 391 (1998) 667.
2. A. Degiron, T.W. Ebbesen, J. Opt. A: Pure Appl. Opt. 7 (2005) S90.

3. F. J. Garcia-Vidal, L.Martín-Moreno, J. B. Pendry, J. Opt. A: Pure Appl. Opt. **7** (2005) S97.
4. K. J. Klein Koerkamp, S. Enoch, F. B. Segerink, N. F. van Hulst, L. Kuipers, Phys. Rev. Lett. 92 (2004) 183901
5. M. Xiao, N. Rakov, J. Phys.: Condens. Matter 15 (2003) L133.
6. R. Gordon, A. G. Brolo, A. McKinnon, A. Rajora, B. Leathem, K. L. Kavanagh, Phys. Rev. Lett. 92 (2004) 037401.
7. H. A. Bethe, Phys. Rev. 66 (1944) 163-182.
8. C. J. Bouwkamp, Philips Res. Rep. 5 (1950) 401.
9. B. Munk, Frequency Selective Surfaces: Theory and Design, John Wiley & Sons, New York, 2000.
10. I. I. Smolyaninov, A. V. Zayats, A. Stanishevsky, C. C. Davis, Phys. Rev. B 66 (2002), 205414.
11. A. V. Zayats, I. I. Smolyaninov, J. Opt. A: Pure Appl. Opt. 5 (2003) S16.
12. E. Popov, M. Nevière, S. Enoch, R. Reinisch, Phys. Rev. B 62 (2000) 16100.
13. L. Martín-Moreno, F. J. García-Vidal, H. J. Lezec, K. M. Pellerin, T. Thio, J. B. Pendry, T. W. Ebbesen, Phys. Rev. Lett. 86 (2001) 1114.
14. A. K. Sarychev, V. M. Shalaev, Phys. Rep. 335 (2000) 275.
15. A. K. Sarychev, V. A. Podolskiy, A. M. Dykhne, V. M. Shalaev, IEEE J. Quant. Electr. 38 (2002) 956.
16. D. J. Bergman, D. Stroud, Solid State Phys., 46 (1992) 14.

Садржај: *Захваљујући томе што им је функционисање засновано на површинским плазмонима, код матрица шупљина субталасних димензија долази до изузетно повећане електромагнетске трансмисије и интензивне локализације поља од неколико редова величине. Због тога су такве структуре предложене као основни градивни блокови за разноврсне примене код којих се користи појачање нелинеарних ефеката. Користећи аналитички приступ, у овом раду пројектовали смо и симулирали матрице субталасних шупљина нанометарских димензија. У нашим експериментима користили смо методу сканирајуће сонде за нанолитографску израду матрица субталасних шупљина у сребрним слојевима спатерованим на супстрату од фотоотпорног позитива. Направили смо правилно распоређене наношупљине различитих облика, распореда и димензија, при чему је ширина најмањих била око 60 nm. Израђене узорке карактерисали смо АФМ микроскопијом.*

Кључне речи: *Нанооптика, површински плазмони, матрице субталасних шупљина, нанофабрикација, нанолитографија, АФМ микроскопија.*